HHS Public Access

Author manuscript

J Neural Eng. Author manuscript; available in PMC 2016 November 30.

Published in final edited form as:

J Neural Eng. 2015 December ; 12(6): 066012. doi:10.1088/1741-2560/12/6/066012.

Local field potential recordings in a non-human primate model of Parkinsons disease using the Activa PC + S neurostimulator

Allison T Connolly[1], **Abirami Muralidharan**[2], **Claudia Hendrix**[2], **Luke Johnson**[2], **Rahul Gupta**[3], **Scott Stanslaski**[4], **Tim Denison**[4], **Kenneth B Baker**[2], **Jerrold L Vitek**[2], and **Matthew D Johnson**[1,5]

[1]Department of Biomedical Engineering, University of Minnesota, USA

[2]Department of Neurology, University of Minnesota, USA

[3]Global Research, Medtronic Neuromodulation, USA

[4]Core Technologies, Medtronic Neuromodulation, USA

[5]Institute for Translational Neuroscience, University of Minnesota, USA

Abstract

Objective—Using the Medtronic Activa® PC + S system, this study investigated how passive joint manipulation, reaching behavior, and deep brain stimulation (DBS) modulate local field potential (LFP) activity in the subthalamic nucleus (STN) and globus pallidus (GP).

Approach—Five non-human primates were implanted unilaterally with one or more DBS leads. LFPs were collected in montage recordings during resting state conditions and during motor tasks that facilitate the expression of parkinsonian motor signs. These recordings were made in the naïve state in one subject, in the parkinsonian state in two subjects, and in both naïve and parkinsonian states in two subjects.

Main results—LFPs measured at rest were consistent over time for a given recording location and parkinsonian state in a given subject; however, LFPs were highly variable between subjects, between and within recording locations, and across parkinsonian states. LFPs in both naïve and parkinsonian states across all recorded nuclei contained a spectral peak in the beta band (10–30 Hz). Moreover, the spectral content of recorded LFPs was modulated by passive and active movement of the subjects' limbs. LFPs recorded during a cued-reaching task displayed task-related beta desynchronization in STN and GP. The bidirectional capabilities of the Activa® PC + S also allowed for recording LFPs while delivering DBS. The therapeutic effect of STN DBS on parkinsonian rigidity outlasted stimulation for 30–60 s, but there was no correlation with beta band power.

Significance—This study emphasizes (1) the variability in spontaneous LFPs amongst subjects and (2) the value of using the Activa® PC + S system to record neural data in the context of behavioral tasks that allow one to evaluate a subject's symptomatology.

john5101@umn.edu.

Keywords

deep brain stimulation; local field potentials; Parkinsons disease; Activa PC + S

Introduction

Abnormal patterns of mesoscale brain activity, detected as local field potentials (LFPs), have been associated with a range of brain disorders (Silberstein *et al* 2003, Hammond *et al* 2007, Kane *et al* 2009) and are increasingly being explored as potential biomarkers for the successful application of pharmacological (Kuhn *et al* 2006) and deep brain stimulation (DBS) (Eusebio *et al* 2011) treatments. Given the relative stability of LFP signal quality over time (Wang *et al* 2014), tools that can detect LFPs from chronically implanted electrodes could also provide new opportunities to investigate longitudinal disease progression in the context of DBS therapy and how LFP features could serve as feedback signals to guide adaptive DBS therapies (Little *et al* 2013) on a subject-specific basis. The recent development (Stanslaski *et al* 2012) and application (Rouse *et al* 2011) of bidirectional interfacing technology, which does not require additional hardware beyond that typically used in DBS surgery, is thus timely.

In this context, it becomes important to gain a deeper understanding of how the spectral content of LFP signals varies with behavior, especially those behaviors that relate to the manifestation of a particular neurological or neuropsychiatric disorder. Such behaviors can be motor as in the case of patients with essential tremor (Koller *et al* 1997), Parkinson's disease (PD) (Burchiel *et al* 1999, Benabid 2003, Deuschl *et al* 2006), and dystonia (Kumar *et al* 1999, Kupsch *et al* 2006). And, they can also be characterized by cognitive processes, fluctuations, or episodes as in cases of obsessive-compulsive disorder (Greenberg *et al* 2006), treatment-refractory depression (Mayberg *et al* 2005, Malone *et al* 2009), epilepsy (Fisher *et al* 2010), pain (Levy *et al* 1987), and addiction (Luigjes *et al* 2012).

Indeed, for studies that have compared LFP recordings across patients diagnosed with (Bronte-Stewart *et al* 2009, Rosa *et al* 2011, Smart *et al* 2015) or animal models rendered to have (Leblois *et al* 2007, Devergnas *et al* 2014, Connolly *et al* 2015) a particular brain disorder, the resting-state recordings have shown an intriguing degree of variability amongst subjects. While the basis for this variability is likely multi-faceted, one major contributing factor is likely to be that symptomatology is often characterized by episodic events, fluctuations in symptoms over time, or symptoms that are not necessarily expressed in resting-state conditions. Thus, in addition to the insights that recording LFP activity longitudinally in a given subject could provide, it is also important to consider the importance of integrating LFP recordings with behavioral context.

Animal studies have shown that the spectral content of LFP signals in the basal ganglia-thalamo-cortical network in rats (Leventhal *et al* 2012) and non-human primates (Sanes and Donoghue 1993, Murthy and Fetz 1996, Courtemanche *et al* 2003) is modulated during the use of a cue and the generation of voluntary movements. Studies in humans have investigated these movement-related LFP oscillations in the context of PD symptoms and therapy (Levy *et al* 2002, Williams *et al* 2003, Kühn *et al* 2004, Alegre *et al* 2005, Doyle *et*

al 2005); however, the experiments have been limited to short periods of time, to the use of tasks that can be performed with the patient seated or reclined in the operating room environment, or to a limited number of patients.

While many behavioral tasks are more suited to study in humans (Rosa *et al* 2013), studies with relatively simple behavioral contexts (e.g. voluntary or cued reaching, passive joint manipulations, or gait dynamics) are well suited to preclinical studies in animal models. These preclinical studies are important in that they can provide data on the consistency of neural recordings over time, which may not be practical in an intraoperative or clinical follow-up setting in humans. Preclinical studies can also provide important insights into the physiological mechanisms of DBS (Hashimoto *et al* 2003, Dorval *et al* 2008, Agnesi *et al* 2013) and translation of new approaches to deliver more robust DBS therapy (Rosin *et al* 2011) that would otherwise not be feasible or be overly tedious to test in patients.

The Activa® PC + S system (Medtronic, Minneapolis, MN) is a chronic implant poised to address these challenges with simultaneous sensing and stimulating capabilities, which enables chronic, untethered recordings from DBS implants (Stanslaski *et al* 2012, Bronte-Stewart *et al* 2014). In this study, we have used this device in five non-human primates to illustrate how the system can be used to investigate mesoscale neural activity within the subthalamic nucleus (STN) and globus pallidus (GP) in the context of several behavior tasks relevant to the expression of parkinsonian motor signs.

Methods

Subjects

Five adult rhesus macaque monkeys (macaca mulatta, G (♀, 9.0 kg, 17 y.o.), F (♀, 8.6 kg, 24 y.o.), L (♀, 6.5 kg, 18 y.o.), M (♀, 6.5 kg, 14 y.o.), and P (♀, 9.5 kg, 19 y.o.)) were used in this study. All procedures were performed in compliance with the United States Public Health Service policy on the humane care and use of laboratory animals, and were approved by the University of Minnesota Institutional Animal Care and Use Committee. Subjects were implanted with 19 mm (inner diameter) cephalic chambers (Crist Instruments, Bethesda, MD) (Elder *et al* 2005). Monkeys were trained to sit quietly with head restrained in a primate chair while recordings were performed. The monkeys were familiarized with a reaching task and were trained to permit passive manipulation of the joints without resisting with voluntary muscle contractions. The subcortical targets were localized using serial microelectrode mapping techniques involving epoxy-insulated tungsten electrodes (impedance 0.8–1.2 MΩ measured at 1 kHz, FHC Inc, Bowdoin, ME). Firing rates and patterns of single neurons along the microelectrode track were used to localize the borders of these nuclei (Miller and DeLong 1987, Filion and Tremblay 1991, Hutchison *et al* 1998). The sensorimotor sub-region of each target nucleus was further identified using passive manipulation of the wrist, elbow, shoulder, ankle, knee, and hip joints to identify neurons responsive to passive movement (DeLong *et al* 1985, Filion *et al* 1989, Agnesi *et al* 2013).

For monkeys F and M, a scaled-down version of the Medtronic 3387 DBS lead consisting of annular contacts (diameter 630 μm, height 500 μm, vertical pitch 1000 μm, NuMed, Hopkinton, NY, four contacts in F, eight contacts in M) was implanted in the STN area

(figure 1(a)). Monkeys L and M were implanted with the same scaled-down lead in the GP (table 1). Monkeys G and P were implanted with two radially segmented DBS arrays (rDBSA, NeuroNexus, Ann Arbor, MI), one in the STN and one in the GP. The rDBSA consisted of eight rows of four elliptical contacts arranged radially around the lead (height 600 μm in GP, 330 μm in STN, width 300 μm, vertical pitch 750 um, radial pitch 90°). All implants were unilateral, and locations of electrode contacts were identified by co-registering post-implant computed tomography scans with pre-operative 3 T /7 T magnetic resonance imaging using *Monkey Cicerone* (Miocinovic *et al* 2007). The monkeys were implanted for 2–24 months prior to the time of LFP recordings.

MPTP injections

Monkeys G, F, L, and P were rendered parkinsonian through intracarotid and intramuscular injections of the neurotoxin 1-methyl-4-phenyl-1,2,3,6-tetrahydropyridine (MPTP, 0.2–0.6 mg kg^{-1}, 1 mg ml^{-1} solution, Sigma Aldrich or Toronto Research Chemicals). The induced parkinsonian state was evaluated using a modified Unified Parkinson's Disease Rating Scale (mUPDRS), which rated parkinsonian motor signs for limb akinesia, bradykinesia, rigidity, tremor, feeding, defense reaction, gait, posture, balance, turning, and food retrieval (mild: 3–13, moderate: 18–28, and severe: 32–42).

LFP Recordings

A non-implanted Activa® PC + S pulse generator with sensing amplifier circuitry was used to record LFPs by connecting the two extension cables to contacts on the implanted DBS leads, while the device casing was grounded to the animal. For each subject, the electrode contacts determined to be in or near the sensorimotor territory of the target nucleus were used for the recordings. Table 1 details the monkey-specific experiments. The Activa® PC + S system records LFPs differentially between two contacts to reduce common noise from movement, electrical stimulation, and far-field electromagnetic sources. In monkeys G and P who were implanted with rDBSAs, individual neighboring contacts in a single row were mechanically coupled to form a virtual-annular contact that could produce voltage fields equivalent to the annular contacts of the DBS leads implanted in monkeys F, L, and M (Keane *et al* 2012). Prior to recording, the monopolar and bipolar impedances were measured using the N'Vision programmer (Model 8840, Medtronic, Minneapolis, MN) to ensure the connections were secure.

LFPs were assessed in the context of spontaneous activity, passive movement, and active movement. Spontaneous neural activity was recorded with the animal awake and sitting quietly in its primate chair. The Activa® PC + S system was capable of recording one time-domain channel per extension cable with a total memory capacity of 1 MB, which allowed for 16 min of recording two simultaneous time-domain channels at 422 Hz (34 min at 200 Hz, 8 min at 800 Hz). A 0.5 Hz high pass filter and 100 Hz low pass filter were implemented on the device to remove baseline drift and hardware noise. By connecting all four contacts on a single extension cable to four contacts on the DBS lead, the montage-recording mode automatically measured 60 s recordings from all combinations of contact pairs in sequence. These montages were repeated on five different days and power spectral densities were averaged over the days. To ensure the Activa® PC + S was able to record a viable signal,

LFPs at rest were also recorded using the Alpha Omega SNR (Alpha Omega, Israel, sampling rate 1.395 kHz) or the TDT RZ2 (Tucker Davis Technologies, Alachua, FL, sampling rate 3.052 kHz) on the same day but not simultaneously. LFPs were referenced to the titanium headpost or cephalic recording chamber. Offline, the signals were re-referenced to replicate the bipolar montage that was recorded by the Activa® PC + S.

After MPTP injection, LFPs were recorded from monkey P while the researcher passively manipulated the joints to assess rigidity for at least 50 repetitions within the same recording session. In monkeys F and L, the Activa® PC + S was used to record bipolar LFPs during the performance of at least 100 trials of a cued-reach task for a liquid reward within the same recording session. The task required the monkey to place its hand on a capacitively-coupled startpad, which output a value of 0 V at baseline and 5 V when a hand was present. After a variable delay (1–1.5 s), a circular target (diameter 10 cm) appeared on a touch screen in 1 of 8 positions whereupon the primate was required to reach and touch the screen within 1 s in order to receive a liquid reward.

The montage mode of the Activa® PC + S system recorded bipolar LFPs from all six pairs of the four electrodes serially, which enabled the researchers to identify the location and spacing of the electrode pair that maximized the signal of interest (figures 1(b) and (c)). If the source of the spectral content were modeled as a single dipole, then the montage recordings could be used to deduce the location of said source. A source located on the plane, directly between the two recording contacts and orthogonal to the lead axis would be canceled out by the differential amplifier and indiscernible in the recordings. However, as the source moved away from the centroid towards one electrode, and in turn away from the other, its amplitude would increase. Similarly, the amplitude of a source of fixed signal strength outside the electrode pair, or ‘far-field’, would decrease as the distance between the source and the electrodes increased.

Recordings during both passive and active movement required synchronization of the Activa® PC + S system with an external motion capture system (Vicon, Centennial, CO; Motion Analysis, Santa Rosa, CA), which monitored limb location using infrared cameras and reflective markers. This involved connecting the DBS contacts in parallel to an external recording system (AlphaOmega SnR and Alphalab; TDT RZ2) and delivering a synchronization signal via several different methods. Prior to passive manipulation, a recording system was connected in parallel to the DBS lead, and the Activa® PC + S pulse generator was programmed to deliver a 10 Hz pulse train at 0.5 V amplitude for 1–2 s as a synchronizing signal for later analysis. The external system was disconnected for the duration of the recording to avoid introducing extraneous artifacts and then reconnected afterwards. The same stimulation was delivered after the passive manipulation trial and recorded by both the Activa® PC + S system and the external system, allowing for synchronization in post-processing. During the cued reaching task, the first Activa® PC + S system time domain channel was connected to two contacts on the DBS lead and the second time domain channel was connected to the startpad through a 1000x voltage divider for continuous syncing between the task and neural activity.

In monkey F, spontaneous LFPs were recorded between C1 and C3 during cathodic stimulation through C2 in reference to the metal casing of the Activa® PC + S pulse generator. The stimulus waveform was a 60 μs long initial pulse, amplitude between 0.6 V and 1.6 V, followed by a 3 ms long charge-balancing anodal pulse, all delivered at a frequency of 180 Hz, for a duration of 30 s. The mUPDRS was measured at each stimulus amplitude and during the ⩾120 s washout between stimulation periods to ensure that parkinsonian rigidity returned to baseline levels prior to initiating the subsequent trial. These recordings were repeated on four separate days.

Data analysis

Data was analyzed offline using custom Matlab scripts (v2014a, Mathworks, Natick, MA) and the Chronux toolbox (Mitra and Bokil 2008). The first two seconds of each recording were trimmed to remove the settling offset imposed by the recording amplifiers. Recordings were then passed through a moving window line noise subtraction algorithm to remove significant 60 Hz sign waves and subsequently detrended to remove continuous noise artifacts and drifting baseline, respectively (Levkov *et al* 1984). Time–frequency analysis was performed using the multitaper method. For spontaneous recordings, spectrograms of the recorded LFPs were calculated using a 2 s wide moving window with 200 ms step size and three tapers, resulting in a 1 Hz multi-tapered frequency resolution. Artifacts were identified based on the spectrogram power averaged over all frequencies. Windows with an average power exceeding a threshold were removed from further analysis. The threshold was initially set to mean plus two standard deviations of the average power over time duration of the recording. Each recording was then visually inspected, and the threshold was adjusted up if the recording contained many movement artifacts. The overall power spectral density (PSD) was calculated by averaging over the remaining spectrogram windows. Bands of interest were defined as low frequencies (<10 Hz), beta (10–30 Hz) and gamma (30–90 Hz).

Offline, LFPs and motion capture data were synchronized in time and resampled to the sampling rate of the external system (2.79 kHz). Periods of continuous cyclic movement were identified in the motion capture data and the joint angle was derived from the position of the joint and its two neighboring joints. The LFP was split into epochs by triggering to the maxima or the minima of this joint angle. LFP epochs containing artifacts as defined above were excluded from further analysis. The spectrogram was calculated for each epoch individually using a 200 ms duration window with 20 ms step and 5 Hz resolution. A control dataset was calculated by artificially choosing 100 trigger times (i.e. angle maxima times) that were randomly selected within the time period of passive manipulation. The mean and standard deviation of the control spectrograms across the randomly selected trigger times were used to normalize each spectrogram triggered to the angle maxima times of the actual passive manipulation motion trajectories.

LFPs recorded during the cued-reaching task were synchronized with the task information and kinematic data offline. The LFP was split into epochs by triggering to (1) the time of cue presentation, (2) the time when the hand left the startpad, or (3) the time when the monkey touched the target. For each epoch, the spectrogram was calculated using a 250 ms duration window with 25 ms steps and 4 Hz resolution. LFP epochs containing artifacts were

excluded. The task spectrograms were compared to a bootstrapped population of spectrograms that were calculated from random trigger points.

For both passive- and active-movement triggered data, a nonparametric cluster permutation test was used to select time–frequency clusters that were significantly different from the bootstrapped data (Maris and Oostenveld 2007). Specifically, the t-value was calculated for each time–frequency sample of the spectrogram and thresholded at a significance level (α = 0.05). Clusters were selected based on time–frequency adjacency using the built-in Matlab function *bwboundaries.m*, and the cluster-level statistic was defined as the sum of the t-values within each cluster. For the cluster with the largest t-value, Monte Carlo random permutation was used to estimate the distribution of the cluster-level statistic. This population was used to calculate the p-value for all clusters, and those with $p < 0.05$ were considered significant.

Data was collected during stimulation on four days. Spectrograms were calculated using a 2 s duration window with no overlap and 1 Hz resolution. For each day, the spectrogram was normalized by subtracting the mean and dividing by the standard deviation of the spectrogram during the initial rest period (stimulation off). Normalized data were combined across days and outliers were identified as points exceeding five standard deviations from the mean and were excluded. To evaluate carryover effects of stimulation, spectrograms were calculated in the 10 s period immediately following stimulation, a 1 s duration window with no overlap was used to increase the number of windows within the short time period. The ANOVA was used to test for the effect of stimulation amplitude on normalized beta band power with a Tukey post-hoc comparison.

Results

Eight DBS leads were implanted in the STN and GP area of five primates (figure 1(a), table 1). While the sensorimotor areas of the nuclei were targeted in all subjects, the relative location of each implanted lead, as determined by alignment of the pre-operative MRI and post-operative CT, varied somewhat across monkeys. All STN leads were implanted using a parasagittal trajectory. A portion of the lead was ventral to the STN in F; the lead was in the medial STN in G, in the lateral STN (sensorimotor territory) but near to the internal capsule in P, and along the posterior margin of STN in M. The leads targeting the GP were implanted on a coronal plane in animals G, L, and P, while the GP lead for monkey M was implanted using a parasagittal trajectory resulting in a more anterior placement of the dorsal electrode contacts along the lead. Histological confirmation of the DBS lead locations were confirmed in monkeys P, G, and M, whereas monkeys F and L remain active on other studies so the implant locations were not confirmed with histology for these two subjects.

Comparison of Activa PC + S recordings to commercial electrophysiological recording systems

LFPs were recorded using three different recording systems, including the Activa® PC + S (table 2). Figure 2 shows example power spectra from the Activa® PC + S and each commercial system. Although the Activa® PC + S had a lower sampling rate, the spectral content was comparable between the Activa® PC + S and the Alpha Omega SNR (AO,

figure 2(a)) and the TDT RZ2 (TDT, figure 2(b)). The content was similar despite the different recording set ups: the Activa® PC + S recorded all LFPs as a bipolar reference between two DBS contacts on the same lead, whereas the commercial systems recorded single ended LFPs between one DBS contact and the far-field headpost. The Activa® PC + S had integrated high-pass filter at 1 Hz and low-pass filter at 100 Hz, which attenuated both low and high frequency power in comparison to the commercial systems. Recording channels that showed a 60 Hz component were consistent across recording systems. Monkey M (naïve) showed little or no beta peak in both types of recordings, indicating the lack of beta in the Activa® PC + S recordings is not due to hardware filters or noise floor. In monkey L (MPTP treated), large beta peaks were seen in both types of recordings, and relative beta amplitudes between montage pairs were consistent across Activa® PC + S and TDT recordings. Some dissimilarities between the Activa® PC + S spectra and the commercial LFPs may be attributed to differences in signal over time and not differences in the systems, as the LFPs were not recorded simultaneously. However, this provided sufficient evidence that the Activa® PC + S could adequately record LFP activity from DBS leads and is useful for chronic electrophysiological studies.

Spontaneous LFP activity as a subject-specific signature

Bipolar LFP montage recordings were performed for all DBS leads while the monkeys were awake and resting in their primate chairs. In the case of recording from all six pairs of the four electrodes serially, a montage recording session was 3–9 min in duration. The montage recordings across nuclei and subjects were highly variable and were more predictive of the individual subject than of the recording location or parkinsonian state (figure 3). A distinctive $1/f^n$ falloff was observed in all recordings and illustrated the low amplitude power in the higher frequencies. The data was filtered into the beta band using a 4th order butterworth filter, and the root mean squared (rms) power was calculated across time. The beta band signal had a median amplitude of 2.6 μV rms with 25% and 75% quantiles of 1.0 and 6.5 μV rms, and the gamma band signal had a median amplitude of 1.5 μV rms and a quantile range of 1.2–3.2 μV rms. The Activa® PC + S had a detectable noise floor of 1 μV rms, which allowed for detection of LFP signal below 100 Hz (Rouse *et al* 2011). Some pronounced spectral content in the beta band was seen in all montages except for that from the GP of monkey M.

In monkeys G and P, montages were recorded in both the naïve and parkinsonian states. For each recording, the $1/f^n$ falloff was estimated by fitting a five parameter nonlinear model $PSD_{model} = A/(C^* F + B)^n + D$ (Connolly *et al* 2015). Then, the beta power was normalized by the power in the gamma band in PSD_{model}. This method adjusted for the variable $1/f^n$ falloff between recordings while avoiding the impact of noise artifacts, such as the 60 Hz line noise or 82 Hz artifact seen in some power spectra in monkeys P and G (figure 3). An ANOVA based on ranked values showed a significant effect of monkey, disease state, and recording nucleus ($F = 138$, $p = 4e-141$) on normalized beta. The rank-sum test showed a significant increase in beta power from the naïve to the parkinsonian state in the STN ($p = 7.54e-17$) and GP ($p = 1.26e-8$) of monkey P. However, beta power decreased in both the STN ($p = 6.05e-36$) and GP ($p = 3.00e-34$) of monkey G. Figure 4 shows PSDs recorded over multiple days from two contact pairs in monkeys F and P. A beta peak was present in

all contact pairs and its shape and size varied between monkeys ($F = 21.56$, $p = 3.36e-5$) as tested by the ranked ANOVA. To test stability in frequency content across recordings, differences between populations of PSDs were tested by using Jackknifing U-statistics (Arvesen 1969). Frequencies above 50 Hz were excluded due to noise artifacts and low signal to noise ratio. Overall frequency content in the 0–50 Hz range varied between monkeys F and P ($p = 0.0012$) and with parkinsonian state in monkey P ($p = 0.0295$). However, U-statistic showed frequency content from the same electrode pair in the same parkinsonian state was not significantly different over multiple recordings ($p = 0.1936$–0.3655).

LFPs were differentially modulated by passive manipulation of the joints

In monkey P, LFPs were recorded while the researcher performed passive manipulation of the arm and leg joints (figure 5). The resting LFP in the STN of monkey P in the parkinsonian state showed a bimodal distribution with a small peak at 10 Hz and a larger, wider peak around 25 Hz (figure 5(b)). The LFP was triggered to the maxima of the elbow, knee, and shoulder angles to visualize manipulation-locked modulations (figure 5(c)). During manipulation of the elbow, there was a decrease at the time of maximum angle followed by an increase in power between 5 and 25 Hz. Manipulation of the knee joint preferentially modulated the 25 Hz activity with a non-significant desynchronization before angle minima followed by a significant synchronization. The shoulder joint modulation only significantly affected frequencies <5 Hz during manipulation of the elbow and wrist but not the ankle.

STN and GP differentially encoded voluntary movement

Monkeys F and L were trained to perform a cued-reaching task during LFP recording. Monkey F performed the task with a reaction time of 375 ± 113 ms (mean ± SD) and a reach time of 449 ± 231 ms. Monkey L had a reaction time of 311 ± 130 msec and a reach time of 353 ± 132 ms. The modulation of LFP oscillations was examined relative to cue presentation, movement onset, and target touch (figure 6). In the STN of monkey F, significant modulations were only observed within or below the beta band frequency range. The beta desynchronization was strongest in the cue-triggered spectrograms and occurred 57 ms following the appearance of the cue. The frequencies <4 Hz showed a strong pre-cue synchronization during the 0.5 s window when the animal was returning to the startpad, followed by a desynchronization during the baseline period. A beta desynchronization was also present in the GP of monkey L and occurred 300 ms following the cue or 100 ms following the start of movement. In addition, synchronization in the low frequencies (<10 Hz) and the gamma bands were also seen at the time of movement onset in the GP. In both the monkeys, synchronization in the beta band followed the time of target touch.

Recording LFPs in the vicinity of DBS

In order to sense LFPs during the delivery of stimulation, the time-domain recording channel was connected to the two contacts surrounding the stimulation contact, which was referenced to the IPG casing and the monkey's headpost (i.e., pseudo-monopolar stimulation). In this manner, the stimulation artifact would be recorded at the same amplitude on each of the sensing contacts and cancel out upon differential amplification. For

monkey F, stimulation was delivered at 180 Hz because it was a therapeutic frequency and produced the smallest spectral artifacts in comparison with 120 Hz and 140 Hz. The therapeutic effect of stimulus amplitude on arm and leg rigidity was determined using mUPDRS (scale of 0–3). Off stimulation, arm and leg rigidity were rated at 2/3. With 0.6 V stimulation, arm rigidity was 1.5/3 and leg rigidity was 2/3. At 1.3 V, arm rigidity was reduced to 0.5/3 and leg rigidity was abolished (0/3). Some rigidity returned at 1.6 V and motor side effects due to stimulation were seen at amplitudes ⩾1.7 V. Side effects resolved immediately when the stimulation was turned off, but the therapeutic effects of stimulation took 30–120 s to wash out.

In monkey F, the Activa® PC + S system was connected to STN 1 (monopolar impedance 2310 Ω) and STN 3 (2304 Ω) for sensing and STN 2 (2618 Ω) for monopolar stimulation. A beta band peak was present in the LFP recorded between STN1 and STN3 without stimulation (figures 7(a)–(c)). This peak persisted during stimulation at sub-therapeutic and therapeutic voltages. A line noise artifact due to the stimulation/sensing hardware interaction was seen at 25 Hz. The amplitude of the normalized beta peak (limited to 10–20 Hz to avoid the 25 Hz noise) during stimulation was significantly correlated with the stimulation amplitude (one-way ANOVA, $F = 22.45$, $p = 1.52e-34$). The Tukey post-hoc test showed stimulation at 0.6–1.9 V significantly increased beta power compared to off stimulation (figure 7(d)). There was also a significant increase in overall power (excluding 25 Hz and 60 Hz because of artifacts) during stimulation ($F = 176$, $p = 1.33e-189$), likely because of stimulation artifact bleeding into the recording due to the slight impedance mismatch of the two sensing electrodes. Post-hoc tests showed significant differences in overall power compared to off stimulation at amplitudes ⩾1.3 V, but not at 0.6 V. The change in beta power could not be separated from this artifact.

Because the stimulation artifact may have influenced the change in normalized beta power seen in the on stimulation case, the effect of stimulation was examined by analyzing the LFP during the 10 s immediately following the termination of stimulation. It was observed that therapeutic effects of stimulation persisted after the end of stimulation for 30–60 s, depending on the stimulation amplitude, although side effects did not persist. However, there was no effect of stimulation amplitude on normalized beta power in the ten seconds following the termination of stimulation ($F = 1.13$, $p = 0.34$, figure 7(e)). The change in beta power seen during stimulation while rigidity was reduced did not persist after the termination of stimulation, even though the improvement in rigidity remained.

Discussion

In this study, we have used the Medtronic Activa® PC + S system to demonstrate the diversity in LFP recordings observable among subjects, implant targets, disease states, and behavioral states. We have shown the Activa® PC + S is capable of recording LFPs from DBS electrodes implanted in the basal ganglia and produces signals comparable to commercial systems. Passive manipulations modulated the spectral content of the LFPs differently in the STN and in the GP and with different joints. This indicates that the LFP is sensitive to receptive fields within these target nuclei. When the monkeys made voluntary movements during a cued-reaching task, the LFPs were strongly time-locked to different

aspects of the movement. A desynchronization was seen in the beta band in both the STN and the GP, but the desynchronization occurred early, near the time of the cue in the STN versus after the time of the movement initiation in the GP.

Technical considerations for recording LFPs from chronically implanted DBS leads

The LFPs presented here were recorded with an externalized device so we could sample neural signals from multiple subjects. When these devices are used in human studies, they are fully implanted, which will reduce artifacts from external noise sources and from movement. This will also ensure a more consistent connection between the DBS leads and the implanted device, which will reduce variability in sensing impedances. However, the impedances will still be subject to changes in the electrode–tissue interface caused by the immune system response, the type of tissue surrounding the electrode, and the delivery of stimulation through specific contacts (Butson *et al* 2006, Lempka *et al* 2009). Impedance matching is critical for sensing in the context of stimulation because the system relies on differential amplification to cancel out the stimulation artifact (Zhang *et al* 2012).

The montage recording mode was a useful tool for demonstrating the subject-specific signature of the LFP spectrum. There was large variability in the power spectra between the two target nuclei in the five monkeys. This heterogeneity has also been demonstrated in human studies (Kuhn *et al* 2005, Bronte-Stewart *et al* 2009, de Solages *et al* 2010). The LFPs did not show trends correlated with parkinsonian disease state across subjects, as beta power increased in monkey P but decreased in monkey G in the parkinsonian compared with the naïve state. In addition, the hypothesized beta biomarker increased during all amplitudes of stimulation, although rigidity was reduced only at DBS between 1.3 and 1.7 V (figure 7). While these results do not point to beta power as a strong biomarker correlated with parkinsonian motor signs across subjects, it does show inter-subject variability consistent with previous non-human primate studies comparing oscillations across parkinsonian states within subjects (Leblois *et al* 2007, Devergnas *et al* 2014, Connolly *et al* 2015). The underlying neural state during spontaneous activity can be influenced by many factors including attention, alertness, and mood. Using the Activa® PC + S to record LFPs in a controlled situation such as a movement or cognitive task may produce statistically stronger and more consistent results across subjects, as was seen in the cued-reaching task studied here (figure 6).

Because the device automatically records from all possible pairs of electrodes, the montage recording mode could be used to understand the baseline spectral content for a specific subject and identify the recording contact pair that yields the most salient biomarker of interest (Zaidel *et al* 2010). The location and spacing of this pair may be informative for diagnosis and stimulation parameter selection (Bour *et al* 2015). However, when comparing the best location and spacing for sensing across subjects, the variability in the location of the lead in the context of the target nuclei must be accounted for. While LFPs varied across animals and between pairs of electrodes, LFPs for a given electrode pair in a given state (e.g. naïve, mild, moderate, severe parkinsonian condition), the LFPs remained fairly consistent from day to day, which indicates that these signals are reliably sensed.

Synchronizing recording of external measures with the LFP is non-trivial and necessary for correlating neural activity with behaviors and symptoms (Ryapolova-Webb *et al* 2014). The exact sampling rate of LFPs by the implantable device could vary compared to external recording systems. For this reason, synchronization at the start and finish of a recording was necessary to precisely align the LFPs with external measures. In this study, the device was externalized which gave us flexibility in the type of signals to be used for synchronization. In a fully implantable device, an external stimulation source such as a transcutaneous electrical nerve stimulation unit could be used to deliver sub-threshold stimulation to the patient's skin, which would induce an artifact on the sensed LFP and could also be recorded by the external system.

LFPs in the context of movement

The motor deficits seen in movement disorders are often state and action dependent (Jankovic, 2008), which suggests that neurophysiological signals should also be studied in the context of different behaviors to understand direct correlates of these motor signs. For example, essential tremor patients show tremor when posturing or moving the limbs, but minimally at rest (Connolly *et al* 2012). Parkinsonian akinesia and freezing of gait are thought to involve interruption in the voluntary generation of movement, so the symptoms themselves are not problematic in a resting state, and therefore perhaps not detectable (Schaafsma *et al* 2003).

The strength and significance of a biomarker of a parkinsonian symptom is also likely to vary based on the nucleus and receptive field from which the LFP is being recorded. As shown in figure 6(b), the timing of an event-related beta desynchronization occurred earlier in the STN than in the GP, which could result from a shorter time delay of the hyper-direct projections from the motor cortex to STN (Nambu *et al* 1996) and from the fact that cortical-striatal activity lags cortico-spinal activity (Turner and DeLong 2000). Movement-locked modulations in the LFP oscillations have been seen in the human STN both unilaterally (Levy *et al* 2002) and bilaterally (Alegre *et al* 2005), in the human peduncolopontine nucleus (Androulidakis *et al* 2008) and in non-human primate striatum (Courtemanche *et al* 2003) and sensorimotor cortex (Murthy and Fetz 1996). Furthermore, modulation in the beta band of the LFP has been shown to be cue-related in the STN of humans (Williams *et al* 2003, Doyle *et al* 2005), in the motor cortex in non-human primates (Sanes and Donoghue 1993), and at multiple locations throughout the basal ganglia-cortical network in rats (Leventhal *et al* 2012). Future studies investigating the relative timing of task-related oscillations across brain networks will need to record LFPs across multiple nuclei in the same subject (de Hemptinne *et al* 2015). The dual-channel recording capability of the Activa® PC + S will make this possible in humans.

Potential of chronic sensing during stimulation

Physiologically optimized DBS, in which a patient's own brain activity is used as the feedback signal to adjust stimulation parameters (Van Gompel *et al* 2010), holds significant promise for patients to obtain a more consistent level of therapy and for clinicians to provide a more efficient method to program a patient's DBS settings. Such approaches are currently in active development for PD (Van Gompel *et al* 2010, Rosin *et al* 2011, Little *et al* 2013,

Priori *et al* 2013), epilepsy (Fountas and Smith, 2007, Morrell, 2011, Sohal and Sun, 2011, Berenyi *et al* 2012, Stanslaski *et al* 2012, Stypulkowski *et al* 2013), and essential tremor (Brittain *et al* 2013, Santaniello *et al* 2011). The present study extends previous application of bi-directional interface hardware in animal models (Rouse *et al* 2011, Afshar *et al* 2012). While closed-loop stimulation has promise, the role of biomarkers in disease state, behavioral context, and therapy level need further scrutiny. Additionally, it is important to consider adapting hardware (Rossi *et al* 2007, Rouse *et al* 2011, Afshar *et al* 2012, Kent and Grill 2012) and software (Sameni *et al* 2007) settings to minimize stimulation artifacts detected in the LFP recordings during DBS. These approaches may further limit the appearance of stimulation artifacts that we observed even though the impedances of each recording electrode were well matched. While the observed increase in spectral power in the beta band during therapeutic STN-DBS in the present study is not consistent with other studies reporting a decrease in beta band power during STN-DBS therapy (Eusebio *et al* 2011, Little *et al* 2013), our findings in one animal are consistent with observations showing that not all subjects exhibit a decrease in beta band activity in the STN area with STN-DBS in the OFF medication state (Giannicola *et al* 2010). While one cannot rule out spectral artifacts related to stimulation contaminating the LFP data fidelity during DBS, the observation that the therapeutic effects of STN-DBS lingered after stimulation but the increased spectral power beta band activity did not linger suggests that the observed spectral changes were not directly related to improvement in rigidity for this subject.

Conclusion

In this study, we used the Medtronic Activa® PC + S neurostimulator (Stanslaski *et al* 2009, Rouse *et al* 2011, Afshar *et al* 2012, Stanslaski *et al* 2012) in a non-human primate model of PD to illustrate how the system can be used, in a range of behavioral contexts, to investigate neural mechanisms of disease and therapy. This data show that mesoscale brain activity sensing from deep brain structures can provide rich electrophysiological databases of subject-specific biomarkers that should be collected in the context of behavior relevant to the expression of symptomatology.

Acknowledgments

This work was supported by research funds from Medtronic, NIH R01 NS-37019, R01 NS077657-02, R01 NS081118; AC was supported by an NSF GRFP (0006595), AM was supported by Parkinson's Disease Foundation Postdoctoral Fellowship for Basic Scientists.

References

Afshar P, et al. A translational platform for prototyping closed-loop neuromodulation systems. Front. Neural Circuits. 2012; 6:117. [PubMed: 23346048]

Agnesi F, Connolly AT, Baker KB, Vitek JL, Johnson MD. Deep brain stimulation imposes complex informational lesions. PLoS One. 2013; 8:e74462. [PubMed: 23991221]

Alegre M, Alonso-Frech F, Rodriguez Oroz M C, Guridi J, Zamarbide I, Valencia M, Manrique M, Obeso JA, Artieda J. Movement-related changes in oscillatory activity in the human subthalamic nucleus: ipsilateral versus contralateral movements. Eur. J. Neurosci. 2005; 22:2315–24. [PubMed: 16262669]

Androulidakis AG, Mazzone P, Litvak V, Penny Dileone M, Gaynor LM, Tisch S, Di Lazzaro V, Brown P. Oscillatory activity in the pedunculopontine area of patients with Parkinson's disease. Exp. Neurol. 2008; 211:59–66. [PubMed: 18282571]

Arvesen JN. Jackknifing U-statistics. Ann. Math. Stat. 1969; 40:2076–100.

Benabid AL. Deep brain stimulation for Parkinson's disease. Curr. Opin. Neurobiol. 2003; 13:696–706. [PubMed: 14662371]

Berenyi A, Belluscio M, Mao D, Buzsaki G. Closed-loop control of epilepsy by transcranial electrical stimulation. Science. 2012; 337:735–7. [PubMed: 22879515]

Bour LJ, Lourens MA, Verhagen R, De Bie RM, Van Den Munckhof P, Schuurman PR, Contarino MF. Directional recording of subthalamic spectral power densities in parkinson's disease and the effect of steering deep brain stimulation. Brain Stimul. 2015; 8:730–41. [PubMed: 25753176]

Brittain JS, Probert-Smith P, Aziz TZ, Brown P. Tremor suppression by rhythmic transcranial current stimulation. Curr. Biol. 2013; 23:436–40. [PubMed: 23416101]

Bronte-Stewart H, Barberini C, Koop MM, Hill BC, Henderson JM, Wingeier B. The STN beta-band profile in Parkinson's disease is stationary and shows prolonged attenuation after deep brain stimulation. Exp. Neurol. 2009; 215:20–8. [PubMed: 18929561]

Bronte-Stewart, H.; Quinn, E.; Blumenfeld, Z.; Velisar, A.; Shreve, L.; Koop, MM.; Kilbane, C.; Rodriguez, C.; Henderson, J.; Hill, B. Movement Disorders. Wiley; NJ, USA: 2014. STN neural synchrony in PD is similar while lying, sitting, standing but different during repetitive movement and walking; p. S432-3.

Burchiel KJ, Anderson VC, Favre J, Hammerstad JP. Comparison of pallidal and subthalamic nucleus deep brain stimulation for advanced Parkinson's disease: results of a randomized, blinded pilot study. Neurosurgery. 1999; 45:1375–82. discussion 1382–4. [PubMed: 10598706]

Butson CR, Maks CB, Mcintyre CC. Sources and effects of electrode impedance during deep brain stimulation. Clin. Neurophysiol. 2006; 117:447–54. [PubMed: 16376143]

Connolly AT, Bajwa JA, Johnson MD. Cortical magnetoencephalography of deep brain stimulation for the treatment of postural tremor. Brain Stimul. 2012; 5:616–24. [PubMed: 22425066]

Connolly AT, Jensen AL, Bello EM, Netoff TI, Baker KB, Johnson MD, Vitek JL. Modulations in oscillatory frequency and coupling in globus pallidus with increasing parkinsonian severity. J. Neurosci. 2015; 35:6231–40. [PubMed: 25878293]

Courtemanche R, Fujii N, Graybiel AM. Synchronous, focally modulated beta-band oscillations characterize local field potential activity in the striatum of awake behaving monkeys. J. Neurosci. 2003; 23:11741–52. [PubMed: 14684876]

de Hemptinne C, Swann NC, Ostrem JL, Ryapolova-Webb ES, San Luciano M, Galifianakis NB, Starr PA. Therapeutic deep brain stimulation reduces cortical phase-amplitude coupling in Parkinson's disease. Nat. Neurosci. 2015; 18:779–86. [PubMed: 25867121]

DeLong MR, Crutcher MD, Georgopoulos AP. Primate globus pallidus and subthalamic nucleus: functional organization. J. Neurophysiol. 1985; 53:530–43. [PubMed: 3981228]

de Solages C, Hill BC, Koop MM, Henderson JM, Bronte-Stewart H. Bilateral symmetry and coherence of subthalamic nuclei beta band activity in Parkinson's disease. Exp. Neurol. 2010; 221:260–6. [PubMed: 19944098]

Deuschl G, et al. A randomized trial of deep-brain stimulation for Parkinson's disease. N. Engl. J. Med. 2006; 355:896–908. [PubMed: 16943402]

Devergnas A, Pittard D, Bliwise D, Wichmann T. Relationship between oscillatory activity in the cortico-basal ganglia network and parkinsonism in MPTP-treated monkeys. Neurobiol. Dis. 2014; 68:156–66. [PubMed: 24768805]

Dorval AD, Russo GS, Hashimoto T, Xu W, Grill WM, Vitek JL. Deep brain stimulation reduces neuronal entropy in the MPTP-primate model of Parkinson's disease. J. Neurophysiol. 2008; 100:2807–18. [PubMed: 18784271]

Doyle LMF, Kühn AA, Hariz M, Kupsch A, Schneider GH, Brown P. Levodopa-induced modulation of subthalamic beta oscillations during self-paced movements in patients with Parkinson's disease. Eur. J. Neurosci. 2005; 21:1403–12. [PubMed: 15813950]

Elder CM, Hashimoto T, Zhang J, Vitek JL. Chronic implantation of deep brain stimulation leads in animal models of neurological disorders. J. Neurosci. Methods. 2005; 142:11–6. [PubMed: 15652612]

Eusebio A, Thevathasan W, Doyle Gaynor L, Pogosyan A, Bye E, Foltynie T, Zrinzo L, Ashkan K, Aziz T, Brown P. Deep brain stimulation can suppress pathological synchronisation in parkinsonian patients. J. Neurol. Neurosurg. Psychiatry. 2011; 82:569–73. [PubMed: 20935326]

Filion M, Tremblay L. Abnormal spontaneous activity of globus pallidus neurons in monkeys with MPTP-induced parkinsonism. Brain Res. 1991; 547:142–51. [PubMed: 1677607]

Filion, M.; Tremblay, L.; Bedard, PJ. Neural Mechanisms in Disorders of Movement. John Libbey; London: 1989. Excessive and unselective responses of medial pallidal neurons to both passive movements and striatal stimulation in monkeys with MPTP-induced parkinsonism.

Fisher R, et al. Electrical stimulation of the anterior nucleus of thalamus for treatment of refractory epilepsy. Epilepsia. 2010; 51:899–908. [PubMed: 20331461]

Fountas KN, Smith JR. A novel closed-loop stimulation system in the control of focal, medically refractory epilepsy. Acta Neurochir. Suppl. 2007; 97:357–62. [PubMed: 17691324]

Giannicola G, Marceglia S, Rossi L, Mrakic-Sposta S, Rampini P, Tamma F, Cogiamanian F, Barbieri S, Priori A. The effects of levodopa and ongoing deep brain stimulation on subthalamic beta oscillations in Parkinson's disease. Exp. Neurol. 2010; 226:120–7. [PubMed: 20713047]

Greenberg BD, Malone DA, Friehs GM, Rezai AR, Kubu CS, Malloy PF, Salloway SP, Okun MS, Goodman WK, Rasmussen SA. Three-year outcomes in deep brain stimulation for highly resistant obsessive-compulsive disorder. Neuropsychopharmacology. 2006; 31:2384–93. [PubMed: 16855529]

Hammond C, Bergman H, Brown P. Pathological synchronization in Parkinson's disease: networks, models and treatments. Trends Neurosci. 2007; 30:357–64. [PubMed: 17532060]

Hashimoto T, Elder CM, Okun MS, Patrick SK, Vitek JL. Stimulation of the subthalamic nucleus changes the firing pattern of pallidal neurons. J. Neurosci. 2003; 23:1916–23. [PubMed: 12629196]

Hutchison WD, Allan RJ, Opitz H, Levy R, Dostrovsky JO, Lang AE, Lozano AM. Neurophysiological identification of the subthalamic nucleus in surgery for Parkinson's disease. Ann. Neurol. 1998; 44:622–8. [PubMed: 9778260]

Jankovic J. Parkinson's disease: clinical features and diagnosis. J. Neurol. Neurosurg. Psychiatry. 2008; 79:368–76. [PubMed: 18344392]

Kane A, Hutchison WD, Hodaie M, Lozano AM, Dostrovsky JO. Enhanced synchronization of thalamic theta band local field potentials in patients with essential tremor. Exp. Neurol. 2009; 217:171–6. [PubMed: 19233174]

Keane M, Deyo S, Abosch A, Bajwa JA, Johnson MD. Improved spatial targeting with directionally segmented deep brain stimulation leads for treating essential tremor. J. Neural Eng. 2012; 9:046005. [PubMed: 22732947]

Kent AR, Grill WM. Recording evoked potentials during deep brain stimulation: development and validation of instrumentation to suppress the stimulus artefact. J. Neural Eng. 2012; 9:036004. [PubMed: 22510375]

Koller W, et al. High-frequency unilateral thalamic stimulation in the treatment of essential and parkinsonian tremor. Ann. Neurol. 1997; 42:292–9. [PubMed: 9307249]

Kuhn AA, Kupsch A, Schneider GH, Brown P. Reduction in subthalamic 8–35 Hz oscillatory activity correlates with clinical improvement in Parkinson's disease. Eur. J. Neurosci. 2006; 23:1956–60. [PubMed: 16623853]

Kuhn AA, Trottenberg T, Kivi A, Kupsch A, Schneider GH, Brown P. The relationship between local field potential and neuronal discharge in the subthalamic nucleus of patients with Parkinson's disease. Exp. Neurol. 2005; 194:212–20. [PubMed: 15899258]

Kühn AA, Williams D, Kupsch A, Limousin P, Hariz Schneider G H, Yarrow K, Brown P. Event-related beta desynchronization in human subthalamic nucleus correlates with motor performance. Brain. 2004; 127:735–46. [PubMed: 14960502]

Kumar R, Dagher A, Hutchison WD, Lang AE, Lozano AM. Globus pallidus deep brain stimulation for generalized dystonia: clinical and PET investigation. Neurology. 1999; 53:871–4. [PubMed: 10489059]

Kupsch A, et al. Pallidal deep-brain stimulation in primary generalized or segmental dystonia. N. Engl. J. Med. 2006; 355:1978–90. [PubMed: 17093249]

Leblois A, Meissner W, Bioulac B, Gross CE, Hansel D, Boraud T. Late emergence of synchronized oscillatory activity in the pallidum during progressive Parkinsonism. Eur J. Neurosci. 2007; 26:1701–13. [PubMed: 17880401]

Lempka SF, Miocinovic S, Johnson MD, Vitek JL, Mcintyre CC. *In vivo* impedance spectroscopy of deep brain stimulation electrodes. J. Neural Eng. 2009; 6:046001. [PubMed: 19494421]

Leventhal DK, Gage GJ, Schmidt R, Pettibone JR, Case AC, Berke JD. Basal ganglia beta oscillations accompany cue utilization. Neuron. 2012; 73:523–36. [PubMed: 22325204]

Levkov C, Michov G, Ivanov R, Daskalov IK. Subtraction of 50 Hz interference from the electrocardiogram. Med. Biol. Eng. Comput. 1984; 22:371–3. [PubMed: 6748774]

Levy R, Ashby P, Hutchison WD, Lang AE, Lozano AM, Dostrovsky JO. Dependence of subthalamic nucleus oscillations on movement and dopamine in Parkinson's disease. Brain. 2002; 125:1196–209. [PubMed: 12023310]

Levy RM, Lamb S, Adams JE. Treatment of chronic pain by deep brain stimulation: long term follow-up and review of the literature. Neurosurgery. 1987; 21:885–93. [PubMed: 3325851]

Little S, et al. Adaptive deep brain stimulation in advanced Parkinson disease. Ann. Neurol. 2013; 74:449–57. [PubMed: 23852650]

Luigjes J, Van den brink W, Feenstra M, Van den Munckhof P, Schuurman PR, Schippers R, Mazaheri A, De Vries TJ, Denys D. Deep brain stimulation in addiction: a review of potential brain targets. Mol. Psychiatry. 2012; 17:572–83. [PubMed: 21931318]

Malone DA Jr, et al. Deep brain stimulation of the ventral capsule/ventral striatum for treatment-resistant depression. Biol. Psychiatry. 2009; 65:267–75. [PubMed: 18842257]

Maris E, Oostenveld R. Nonparametric statistical testing of EEG- and MEG-data. J. Neurosci. Methods. 2007; 164:177–90. [PubMed: 17517438]

Mayberg HS, Lozano AM, Voon V, Mcneely HE, Seminowicz D, Hamani C, Schwalb JM, Kennedy SH. Deep brain stimulation for treatment-resistant depression. Neuron. 2005; 45:651–60. [PubMed: 15748841]

Miller, WC.; DeLong, MR. Altered tonic activity of neurons in the globus pallidus and subthalamic nucleus in the primate MPTP model of Parkinsonism. In: Carpenter, MB.; Jayaraman, A., editors. Basal Ganglia II. Plenum; New York: 1987.

Miocinovic S, Noecker A, Maks C, Butson C, Mcintyre CC. Cicerone: stereotactic neurophysiological recording and deep brain stimulation electrode placement software system. Acta Neurochir. Suppl. 2007; 97:561–7. [PubMed: 17691348]

Mitra, P.; Bokil, H. Observed Brain Dynamics. Oxford University Press; New York: 2008.

Morrell MJ. Responsive cortical stimulation for the treatment of medically intractable partial epilepsy. Neurology. 2011; 77:1295–304. [PubMed: 21917777]

Murthy VN, Fetz EE. Oscillatory activity in sensorimotor cortex of awake monkeys: synchronization of local field potentials and relation to behavior. J. Neurophysiol. 1996; 76:3949–67. [PubMed: 8985892]

Nambu A, Takada M, Inase M, Tokuno H. Dual somatotopical representations in the primate subthalamic nucleus: evidence for ordered but reversed body-map transformations from the primary motor cortex and the supplementary motor area. J. Neurosci. 1996; 16:2671–83. [PubMed: 8786443]

Priori A, Foffani G, Rossi L, Marceglia S. Adaptive deep brain stimulation (aDBS) controlled by local field potential oscillations. Exp. Neurol. 2013; 245:77–86. [PubMed: 23022916]

Rosa M, et al. Pathological gambling in Parkinson's disease: subthalamic oscillations during economics decisions. Mov. Disord. 2013; 28:1644–52. [PubMed: 23554027]

Rosa M, Giannicola G, Servello D, Marceglia S, Pacchetti C, Porta M, Sassi M, Scelzo E, Barbieri S, Priori A. Subthalamic local field beta oscillations during ongoing deep brain stimulation in

Parkinson's disease in hyperacute and chronic phases. Neurosignals. 2011; 19:151–62. [PubMed: 21757872]

Rosin B, Slovik M, Mitelman R, Rivlin-Etzion M, Haber SN, Israel Z, Vaadia E, Bergman H. Closed-loop deep brain stimulation is superior in ameliorating parkinsonism. Neuron. 2011; 72:370–84. [PubMed: 22017994]

Rossi L, Foffani G, Marceglia S, Bracchi F, Barbieri S, Priori A. An electronic device for artefact suppression in human local field potential recordings during deep brain stimulation. J. Neural. Eng. 2007; 4:96–106. [PubMed: 17409484]

Rouse AG, Stanslaski SR, Cong P, Jensen RM, Afshar P, Ullestad D, Gupta R, Molnar GF, Moran DW, Denison TJ. A chronic generalized bi-directional brain-machine interface. J. Neural Eng. 2011; 8:036018. [PubMed: 21543839]

Ryapolova-Webb E, Afshar P, Stanslaski S, Denison T, De Hemptinne C, Bankiewicz K, Starr PA. Chronic cortical and electromyographic recordings from a fully implantable device: preclinical experience in a nonhuman primate. J. Neural. Eng. 2014; 11:016009. [PubMed: 24445430]

Sameni R, Shamsollahi MB, Jutten C, Clifford GD. A nonlinear Bayesian filtering framework for ECG denoising. IEEE Trans. Biomed. Eng. 2007; 54:2172–85. [PubMed: 18075033]

Sanes JN, Donoghue JP. Oscillations in local field potentials of the primate motor cortex during voluntary movement. Proc. Natl Acad. Sci. USA. 1993; 90:4470–4. [PubMed: 8506287]

Santaniello S, Fiengo G, Glielmo L, Grill WM. Closed-loop control of deep brain stimulation: a simulation study. IEEE Trans. Neural Syst. Rehabil. Eng. 2011; 19:15–24. [PubMed: 20889437]

Schaafsma JD, Balash Y, Gurevich T, Bartels AL, Hausdorff JM, Giladi N. Characterization of freezing of gait subtypes and the response of each to levodopa in Parkinson's disease. Eur. J. Neurol. 2003; 10:391–8. [PubMed: 12823491]

Silberstein P, et al. Patterning of globus pallidus local field potentials differs between Parkinson's disease and dystonia. Brain. 2003; 126:2597–608. [PubMed: 12937079]

Smart OL, Tiruvadi VR, Mayberg HS. Multimodal approaches to define network oscillations in depression. Biol. Psychiatry. 2015; 77:1061–70. [PubMed: 25681871]

Sohal VS, Sun FT. Responsive neurostimulation suppresses synchronized cortical rhythms in patients with epilepsy. Neurosurg. Clin. N. Am. 2011; 22:481–8. [PubMed: 21939847]

Stanslaski S, Afshar P, Cong P, Giftakis J, Stypulkowski P, Carlson D, Linde D, Ullestad D, Avestruz AT, Denison T. Design and validation of a fully implantable, chronic, closed-loop neuromodulation device with concurrent sensing and stimulation. IEEE Trans. Neural. Syst. Rehabil. Eng. 2012; 20:410–21. [PubMed: 22275720]

Stanslaski S, Cong P, Carlson D, Santa W, Jensen R, Molnar G, Marks WJ Jr, Shafquat A, Denison T. An implantable bi-directional brain-machine interface system for chronic neuroprosthesis research. Proc. Conf. IEEE Eng. Med. Biol. Soc. 2009:5494–7.

Stypulkowski PH, Stanslaski SR, Denison TJ, Giftakis JE. Chronic evaluation of a clinical system for deep brain stimulation and recording of neural network activity. Stereotact. Funct. Neurosurg. 2013; 91:220–32. [PubMed: 23548876]

Turner RS, DeLong MR. Corticostriatal activity in primary motor cortex of the macaque. J. Neurosci. 2000; 20:7096–108. [PubMed: 10995857]

Van Gompel JJ, Chang SY, Goerss SJ, Kim IY, Kimble C, Bennet KE, Lee KH. Development of intraoperative electrochemical detection: wireless instantaneous neurochemical concentration sensor for deep brain stimulation feedback. Neurosurg. Focus. 2010; 29:E6.

Wang D, Zhang Q, Li Y, Wang Y, Zhu J, Zhang S, Zheng X. Long-term decoding stability of local field potentials from silicon arrays in primate motor cortex during a 2D center out task. J. Neural. Eng. 2014; 11:036009. [PubMed: 24809544]

Williams D, Kuhn A, Kupsch A, Tijssen M, Van Bruggen G, Speelman H, Hotton G, Yarrow K, Brown P. Behavioural cues are associated with modulations of synchronous oscillations in the human subthalamic nucleus. Brain. 2003; 126:1975–85. [PubMed: 12847073]

Zaidel A, Spivak A, Grieb B, Bergman H, Israel Z. Subthalamic span of β oscillations predicts deep brain stimulation efficacy for patients with Parkinson's disease. Brain. 2010; 133:2007–21. [PubMed: 20534648]

Zhang F, Holleman J, Otis BP. Design of ultra-low power biopotential amplifiers for biosignal acquisition applications. IEEE Trans. Biomed. Circuits Syst. 2012; 6:344–55. [PubMed: 23853179]

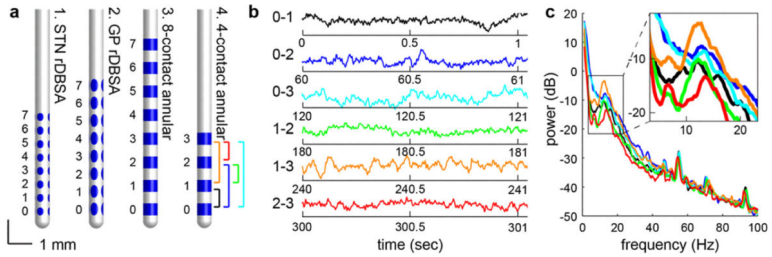

Figure 1.

(a) Four types of DBS leads were implanted in the five monkeys, denoted as leads 1–4 (here, and in subsequent figures). (b) Example LFP snippets from a single 60 s montage recording are shown from monkey F using lead 4. LFPs were sampled from each pair of leads in series, 0–1 (black), 0–2 (blue), 0–3 (cyan), 1–2 (green), 1–3 (orange), and 2–3 (red). Corresponding PSDs are shown in (c), and the inset highlights the variability in the spectral peak.

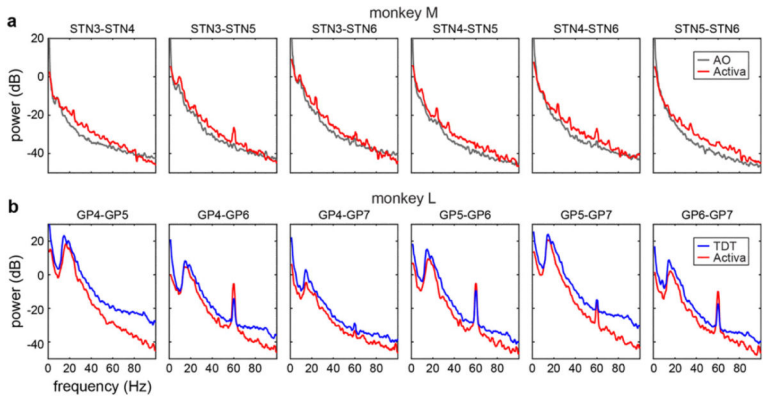

Figure 2.

The LFP frequency content measured with the Activa® PC + S (red) and with commercial systems taken on the same day. LFPs were recorded from a DBS lead in the subthalamic nucleus (STN) of monkey M using the Alpha Omega SNR (AO, gray) and the Activa® PC + S (a). LFPs were recorded from a DBS lead in the globus pallidus (GP) of monkey L using the Tucker Davis Technologies RZ2 (TDT, blue) and with the Activa® PC + S (b).

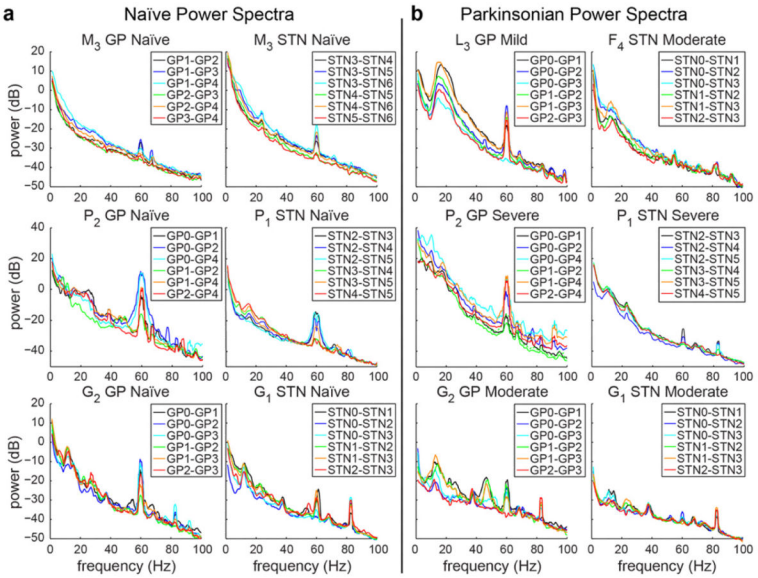

Figure 3.

Average power spectral densities across multiple montages for each DBS lead in each monkey. (a) PSDs recorded in the naïve state are on the left and (b) PSDs recorded after administration of MPTP are on the right. The subscript indicates the type of DBS lead implanted in the subject.

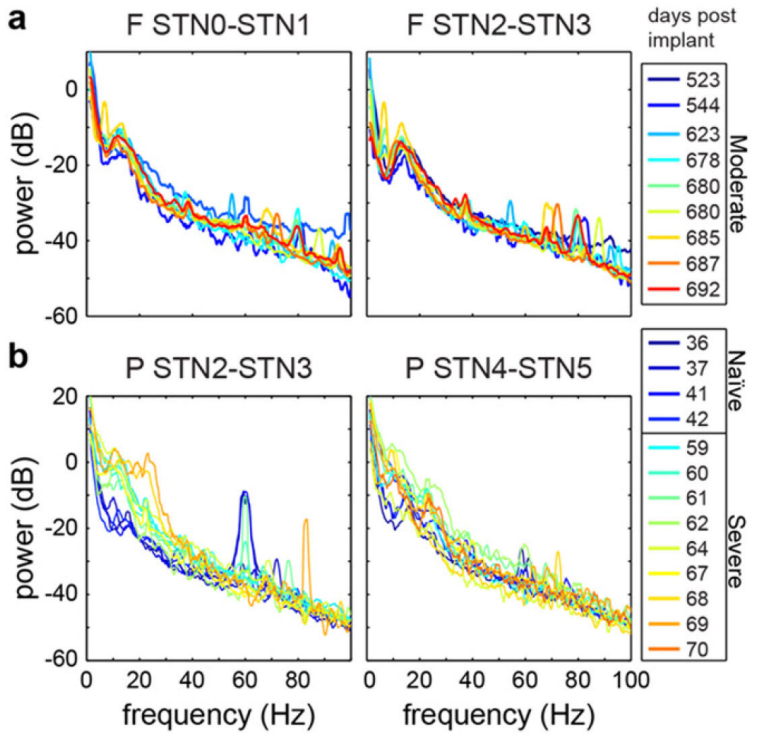

Figure 4.

LFP frequency content was consistent across multiple recording sessions in monkey F (a) and monkey P (b). Spectral content differed between recording contacts in the same monkey, between monkeys, and between parkinsonian states.

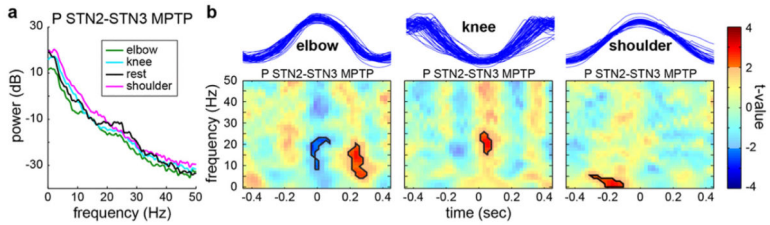

Figure 5.

LFPs recorded from monkey P during passive manipulation of the joints. Spectrograms show spectral changes that depended on the phase of the joint movement. (a) PSDs for one contact pair in the STN during manipulation of the joints. (b) Spectrograms of LFPs triggered to the maxima/minima of the joint angle during manipulation of the elbow, knee, and shoulder. Black outlined regions show time–frequency clusters that were significantly different from a bootstrapped population.

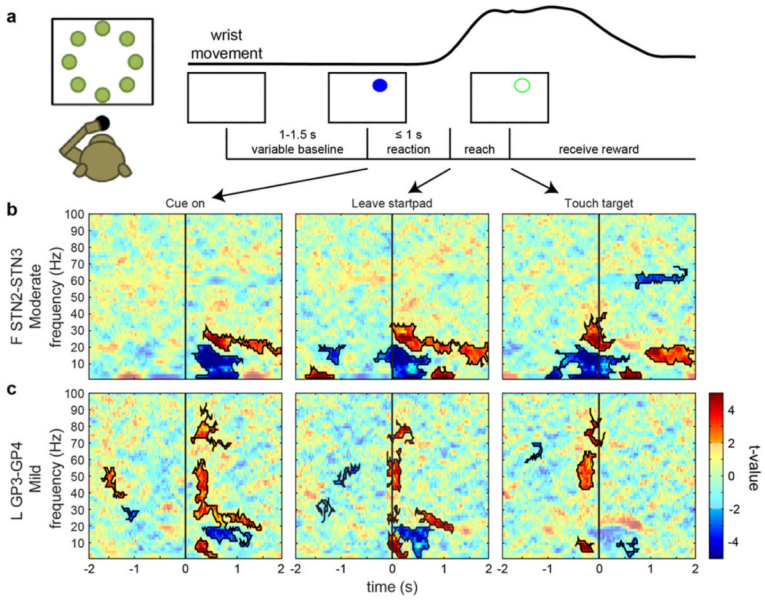

Figure 6.

LFPs recorded from monkeys F and L during 278 and 194 trials of a cued-reaching task, respectively. (a) The task required the monkey to place its hand on a startpad and wait for a variable 1–1.5 s. After the presentation of a cue/target (blue circle) in a random location, the monkey reached out and touched the cue/target (green) and received a reward. (b), (c) For monkeys F and L, respectively, color plots show spectral modulation triggered to the time of cue presentation (left), the time when the hand left the startpad (middle), and the time when the target was touched (right) relative to the variable baseline. Synchronization relative to baseline was colored yellow/red and desynchronization was colored blue. Black outlined regions show time–frequency clusters that were significantly different from a bootstrapped population.

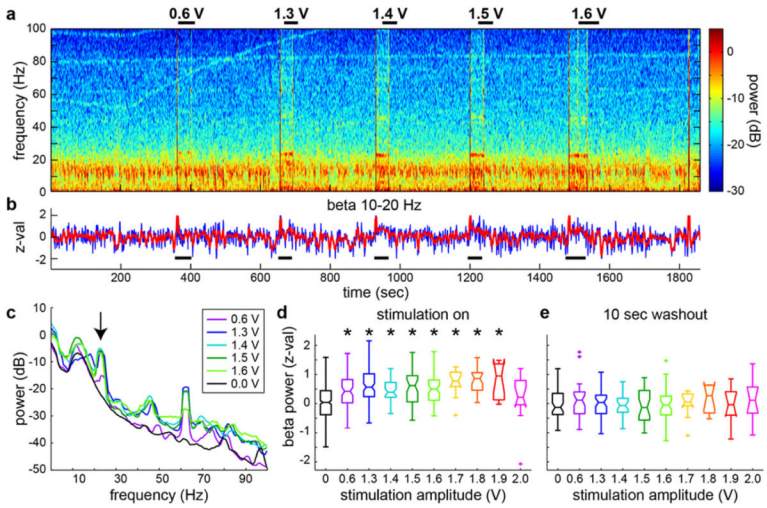

Figure 7.

LFPs recorded from monkey F STN1-STN3 during monopolar stimulation through STN2 at rest. (a) Spectrogram of the LFP with stimulation off, during stimulation at increasing amplitudes (black bars), and during washout times. (b) The blue trace shows beta power (10–20 Hz) normalized by the power at rest before stimulation, and the red trace is the normalized beta power smoothed with a 5 s window. (c) PSD at baseline (black) and during stimulation at increasing amplitudes (colors) showed a spectral peak in the beta band (10–20 Hz) and a stimulation artifact at 25 Hz (arrow). (a)–(c) Data from a single day. (d) Boxplots of normalized beta power at increasing stimulation amplitudes recorded across four days. Asterisks (*) indicate conditions significantly different from stimulation off (0 V), as determined by an ANOVA and Tukey post-hoc test based on ranks. (e) Boxplots of normalized beta power during the 10 s washout period immediately following stimulation at increasing amplitudes.

Table 1

Details of DBS implant type, location, and experiments conducted in each monkey. The monkeys recorded were rendered systemically (S) or hemi-(H) parkinsonian with MPTP. PM: passive movement; CRT: cued-reaching task. Experiments were repeated over multiple days (*d*) and trials (*t*) as indicated by parentheses.

			Disease State		Experiment		
Monkey ID	**GP Lead Type**	**STN Lead Type**	**Naïve**	**Parkinsonian**	**Spontaneous**	**PM**	**CRT**
G	1	2	X	X–S	X (*d* = 12)	—	—
F	—	4	—	X–H	X (*d* = 9)	—	X (*t* = 278)
M	3	3	X	–	X (*d* = 4)	—	—
L	3	—	—	X–H	X (*d* = 3)	—	X (*t* = 194)
P	1	2	X	X–S	X (*d* = 13)	X (*t* = 89)	—

Table 2

Specifications of the recording systems compared in this study (Rouse *et al* 2011).

	Medtronic Activa® PC + S	**Alpha Omega SNR**	**Tucker-Davis RZ2 & PZ5**
Highpass filter	0.5 Hz	0.075 Hz	0.4 Hz
Lowpass filter	100 Hz	10 kHz	7 kHz
Sampling rate	800 Hz max, 422 Hz LFP	44 kHz max, 1.395 kHz LFP	25 kHz max, 3.052 kHz LFP
Input impedance	1MΩ	100 GΩ	1 GΩ
Input range	±10 V	±62.5 mV	±500 mV
Noise floor	Minimum signal to detect 1 μVrms differential with a noise floor <300 nV/√Hz	5 μVrms single ended	3 μVrms single ended 0.75 μVrms differential